Coupling Reduced Order Models via Feedback Control for 3D Underactuated Bipedal Robotic Walking

Xiaobin Xiong and Aaron D. Ames

Abstract— This paper presents a feedback control methodology for 3D dynamic underactuated bipedal walking, that couples an actuated spring-loaded-inverted-pendulum (aSLIP) for forward walking and the passive Linear Inverted Pendulum (LIP) for lateral balancing. The applications of the reduced order models are twofold. First, we utilize aSLIP optimization to design optimal leg length and angle trajectories, and use the LIP dynamics to find desired boundary condition for lateral roll. Second, we present two feedback stabilization laws which are based on the reduced order models and applied on the full robot to stabilize the sagittal walking and lateral balancing separately. The ultimate feedback controller on the full order 3D walking robot is implemented via control Lyapunov function based Quadratic Programs (CLF-QPs). In particular, the reduced order models are used to approximate the underactuated dynamics and plan desired trajectories that are tracked via CLF-QPs. The end result is 3D underactuated walking, demonstrated in simulation on the bipedal robot Cassie.

I. INTRODUCTION

3D dynamic robotic walking remains an unsolved problem in locomotion research community. On the feedback control side, the difficulties come from the complex nonlinear dynamics, high dimensionality and the intrinsic hybrid nature of the behavior itself. Approximation of the dynamics and control by simple reduced order models has been one of the popular approaches. Canonical simple models, such as the Linear Inverted Pendulum (LIP) [1], [2] and its variants, utilize the integrable nature of the linear dynamics for online motion planning. The planned trajectory is then enforced through the robot's center of mass (CoM). Such implementation requires foot-actuated robots moving with relatively small velocities, so that the zero-moment-point [1] constraint remains valid, i.e. that the LIP approximation is valid.

Another simple model, the spring-loaded-inverted-pendulum (SLIP) model [3], [4], [5], [6], also has been investigated for controlling legged hopping [7], running [8] and walking [9]. Since the dynamics of the energy conserving SLIP offers templates for locomotion behaviors, [6], [10] embedded the SLIP dynamics on the CoM of planar robots. Due to the energy loss of ground impact and model difference, energy stabilization [7], [6] and stepping stabilization methods [9], [4] have been applied to stabilize the system dynamics. Consequently, adding actuation on the SLIP model [7], [9] becomes necessary.

Actuation of the SLIP model is normally done by varying leg length [9] or applying force actuation in the leg [7].
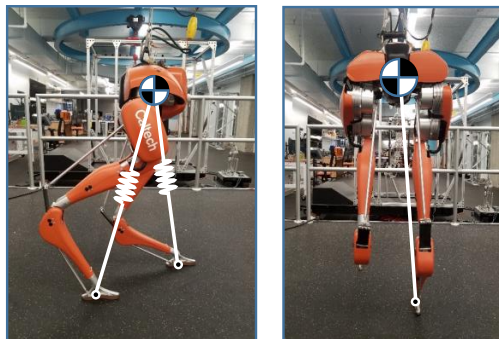
Fig. 1. The actuated SLIP model in the sagittal plane (left) and the LIP model in the lateral plane (right).

Faithful connection between the actuated SLIP model and the full order robot oftentimes is missing. We posit that the connection becomes important when the reduced order models are applied on underactuated robots [10], [11]. Our recent work on bipedal hopping [12] has indicated this as well. The underactuation of the compliance can be approximated by that of the spring in the SLIP subject to the actuated part of the robot, i.e. the leg length. To better understand of the approximation of complex robots via simple models, this paper presents a methodology for 3D underactuated walking control using simple planar models.

The reduced order models are an actuated SLIP (aSLIP) and an underactuated LIP. The aSLIP is an application of our discovery of the nonlinear leg spring approximation [12] for the compliant robot Cassie. The approximation relies on the fact that the spring dynamics dominates the dynamics contribution of the leg to the upper part of the robot. Continuing from the success of the hopping, we present the periodic walking behavior of the leg spring approximation in the form an aSLIP walking in the sagittal plane. The lateral balancing becomes a nontrivial problem for underactuated feet and, as such, we present a feedback stepping method based on the LIP approximation of the lateral dynamics. This is partially inspired by [11], in which the LIP dynamics is used for controlling a single domain walking of a point footed robot. The difference lies in our consideration of two domain walking and compliant foot ground contact.

The planar models provide the feedback-planned trajectories for the underactuated walking. The control Lyapunov function based Quadratic program (CLF-QP) [13] is utilized for trajectory tracking. The final result is a feedback controller that achieves 3D underactuated walking, as is demonstrated in simulation on a full-order model of Cassie.

II. ROBOT MODEL

In this section, we describe the robot model and leg spring model based on the physical robot Cassie [14], [12]. The main characteristics of this robot is the compliant springs in the leg, which facilities a strong correlation between the SLIP model and the physical robot [15], [12]. It is important to note that: despite the fact that our model is specific to this robot, the feedback planning and control is general for robots with leg compliance and foot underactuation. This comes from the application of reduced order models, which will be explained in later sections.

A. Kinematics and Dynamics Model

The robot Cassie is designed with five motor joints, two compliance leaf springs and two closed kinematic chains in each leg. Fig. 2 shows the links and joints on one leg. The toe (foot) of the leg is very narrow, thus we model it as a line segment, which introduces foot rolling during ground contact. The leaf springs are modeled as torsional springs, the stiffness and damping of which are provided by the robot manufacturer [14]. The closed kinematic chains are connected by lightweight aluminum rods. To simplify the closed chain dynamics, we replace the achilles rods by holonomic constraints between the connectors [12] and remove the plantar rods by placing the toe actuation at the toe pitch joints directly. The resultant leg model has 2 spring joints, 1 passive tarsus joint and the 5 motor joints. Using the floating base model, we present the Euler-Lagrange equation with holonomic constraints:

$$M(q)\ddot{q} + H(q,\dot{q}) = Bu + J_s^T \tau_s + J_{h,v}^T F_{h,v}, \quad (1)$$

$$J_{h,v}(q)\ddot{q} + \dot{J}_{h,v}(q)\dot{q} = 0, \quad (2)$$

where $q \in SE(3) \times \mathbb{R}^{n=16}$, $M(q)$ is the mass matrix, $H(q,\dot{q})$ is the Coriolis, centrifugal and gravitational term, B and $u \in \mathbb{R}^{10}$ are the actuation matrix and the motor torque vector, τ_s and J_s are the spring joint torque vector and the corresponding Jacobian, and $F_{h,v} \in \mathbb{R}^{n_{h,v}}$ and $J_{h,v}$ are the holonomic force vector and the corresponding Jacobian respectively. We use subscript v to indicate different domains. For example, when robot has two feet contacting the ground, i.e. in Double Support Phase (DSP), $n_{h,v=\text{DSP}} = 12$ (2 holonomic constraints by achilles rods and 5 by each foot contact).

B. Leg Spring

Since the robot is designed with lightweight legs and compliant springs in the leg, we use the leg spring to approximate the leg compliance. Our previous work that achieved hopping on Cassie [12] indicates that the compliance of the shin and tarsus springs can be approximated by a nonlinear prismatic spring along the leg direction, i.e. leg spring. The stiffness of the leg spring is similar to the end-effector stiffness of parallel robotic manipulators; the closed kinematic chain in the robot leg makes it to resemble a parallel robotic manipulator. We refer the readers to [12] for detailed derivations of the leg spring for the robot. This results in polynomial
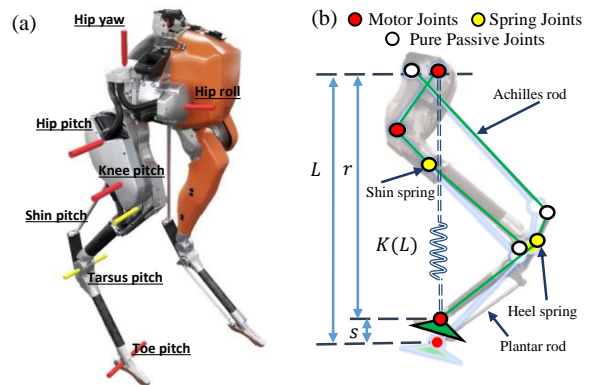

Fig. 2. The leg joints (a) and the leg model (b) of the robot Cassie. The real leg length r is the distance between the hip pitch joint to the tow pitch joint. The leg length L is the real leg length when the spring deflections are zero.

regressions to approximate the stiffness and damping of the leg spring as functions of the leg length L. Consequently, the stiffness K of the leg spring is calculated as,

$$K(L) = \beta_0 + \beta_1 L + \beta_2 L^2 + \beta_4 L^4, \quad (3)$$

where β_i are the coefficients from the polynomial regression. The damping $D(L)$ of the leg spring is approximated in the same way. The leg spring force is written as,

$$F = K(L)s + D(L)\dot{s}. \quad (4)$$

where $s, \dot{s}$ are the spring deformation and deformation rate. By the definition of leg length L (see Fig. 2), $s = L - r$, which is a holonomic constraint. The leg spring has shown to capture the axial dynamics of the system [12]. Inspired by this, we present the planar actuated Spring-Loaded-Inverted-Pendulum (aSLIP), which will be used for trajectory generation and feedback control for the full robot.

III. THE aSLIP MODEL FOR FORWARD WALKING

The canonical SLIP model consists a point mass attaching on mass-less linear springs with certain normal leg length and spring stiffness [3], [5]. In biomechanics community, this simple model has been used to understand the dynamics of human walking [3]. In robotic locomotion, it has also inspired robot designs [15], [8] and control methodologies [6], [8], [10] based on the dynamics behavior of the SLIP.

Our aSLIP model uses the leg spring to replace the linear spring and use the pelvis as the point mass. The leg spring dynamics is affected by the leg length actuation, so is the point mass. As a result, our aSLIP model differs from the canonical SLIP models in the following ways. First, our leg spring is a nonlinear spring. Second, damping of the spring is not neglected so that active control is necessary for energy compensation. Third, the actuation is included by changing of the leg length.

In this section, we first present the dynamics of the aSLIP. Then the trajectory generation method via direct collocation is described to generate optimal trajectories for walking. Lastly, we present a feedback control law to stabilize optimized trajectories on the aSLIP model to enable walking.

A. Dynamics of the aSLIP Walking

The aSLIP model of locomotion is a dynamic hybrid phenomenon, the domains of which differentiate by the number of contacts. The walking can be generally described as a periodic alternation of Single Support Phase (SSP) and Double Support Phase (DSP). In both domains, the point mass dynamics can be compactly written as,

$$m\ddot{\mathbf{r}} = \sum \mathbf{F} + m\mathbf{g} \tag{5}$$

where $\mathbf{r} = [x, z]^T$ is the position of the point mass, $\mathbf{F}$ are the leg spring forces, and $\mathbf{g}$ is gravitational vector. For our aSLIP model, the spring forces couple with the leg internal holonomic constraints and leg length actuation. It is preferable to write the system dynamics in polar coordinates. For instance, the dynamics in SSP is,

$$\ddot{r} = \frac{F}{m} - g\cos(\beta) + r\dot{\beta}^2$$
$$\ddot{\beta} = \frac{1}{r}(-2\dot{\beta}\dot{r} + g\sin(\beta))$$
$$\ddot{s} = \ddot{L} - \ddot{r}$$

where β is the leg angle, s is the leg spring deformation, L is the leg length, and r is the distance between the point mass and the point of contact, i.e. the real leg length. F is calculated by (4). We view $\ddot{L}$ as the virtual input to this system. Fig. 3 (a) shows the aSLIP model with all the leg parameters in SSP.

B. Trajectory Optimization via Direct Collocation

Since the system energy dissipates through spring damping, certain ways of energy injection are needed for enabling periodic walking. Energy stabilization methods have been developed in [6], [7] to enforce the system dynamics evolution to be that of an energy conserving SLIP model. Then forward simulation of the energy conserving SLIP model is required to find stable periodic orbits. [9] applied a fixed parameterization of leg length actuation to inject energy explicitly. These methods may lead to over constraining of the system and require parameter finding, and there is a lack of optimality. Here we apply a trajectory optimization via direct collocation method [16] to find optimal periodic solution for the aSLIP walking. The energy injection is encoded implicitly through the optimized leg length actuation.

Our discretization and integration methods are the same as [17], [12]; an even nodal spacing is used for discretizing the trajectory in time for each domain, and the defect constraints is described algebraically by implicit trapezoidal method. As we are interested in periodic walking, continuity of states between domains are enforced. It is desirable to minimize the virtually consumed energy by defining the cost as [1],

$$J_{\text{walking}} = \sum \int_0^{T_i} (\ddot{L}_1^i(t)^2 + \ddot{L}_2^i(t)^2)dt. \tag{6}$$

Additional constraints include the step length, leg length and spring deformation limits, nonnegative spring forces, domain duration and etc.

---

[1] T_i is the duration of each domain. The integration is implemented as summations of trapezoidal integrations for all the domains.
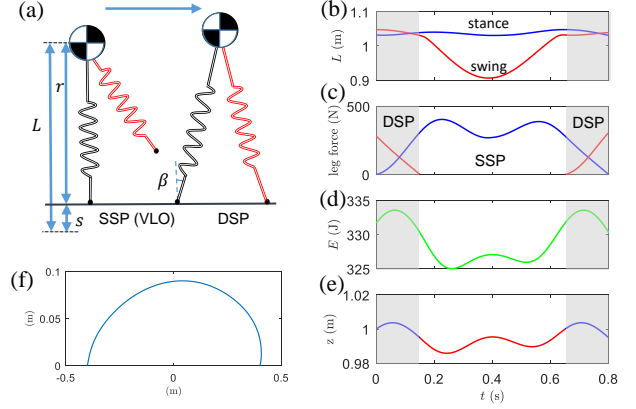

Fig. 3. The aSLIP walking (a) and the optimization results, i.e. (b) the leg length trajectories, (c) spring force profile, (d) energy profile, (e) vertical mass position and (f) the swing foot trajectory.

VLO. We also constrain the states at the time of Vertical Leg Orientation (VLO) [5] with an eye towards the feedback control, which will be explained later. The VLO is the configuration that the stance leg angle is 0 during SSP (Fig. 3(a)), the constraint of which is,

$$\dot{L}_{\text{VLO}} = 0 \tag{7}$$

In implementation, we divide the SSP domain into one before VLO, SSP_{pre}, and one after the VLO, SSP_{post}, so that the VLO states can be directly constrained. Additional constraints also include $L \geq L_{\text{VLO}}$ in SSP_{post} so that energy injection mainly happens in this domain.

Swing Leg Trajectory in SSP. The swing leg trajectory is oftentimes neglected in SLIP walking since it doesn't have dynamics. The swing leg trajectories on the full robot then need to be constructed from the boundary conditions. Here, we construct the swing leg state trajectories from the optimization so that continuity of leg length trajectories $L(t)$ and leg angle trajectories $\beta(t)$ can be directly enforced. The leg spring deformation on the swing leg is assumed to converge to 0 quickly, e.g. $\ddot{s}_2 = -K(L)s_2 - D(L)\dot{s}_2$ can serve this need. The kinematic constraint $L_2 = s_2 + r_2$ is also enforced. Desired swing foot height is constructed by a half sinusoidal curve. Note that both the swing leg angle and length trajectories are useful for the full robot. For controlling the aSLIP model, the swing leg angle trajectory can be used or ignored, depending on the switching conditions.

Fig. 3 shows one optimization result for a walking gait with $T_{\text{SSP}} = 0.5s, T_{\text{DSP}} = 0.15s$. Note that the optimization for periodic walking is performed only once.

C. Feedback Control on aSLIP

Stabilization of the optimized trajectories is commonly done by feedback control on the output dynamics [16], [18]. For underactuated walking, periodic stability is then checked through Poincaré maps [19]. Typically, only stable trajectories are used [16], [18]. Due to the hybrid nature of walking, additional stabilization schemes focus on utilizing

the discrete transition, including adjusting touch down angle [8] and step length [18].

For our aSLIP model, we tried the abovementioned stabilization methods, using feedback control to track the desired output trajectories $[L(t); \dot{L}(t)]^2$ with touch down angle or step length modulations. The resultant stability of the closed loop system still depends on the trajectory optimization results. In other words, not all reasonable optimized trajectories can be stabilized. Inspired by [5] of developing Poincaré section at the VLO configuration, we discover the following feedback modulation on the leg length trajectory based on the VLO velocity:

$$L_d = L_{\text{VLO}} + \Gamma \Delta L \qquad (8)$$
$$\dot{L}_d = \Gamma \dot{L} \qquad (9)$$

with,

$$\Delta L = L - L_{\text{VLO}} \qquad (10)$$
$$\Gamma = 1 - K_p(v_{\text{vho}} - v_{\text{vho}}^{\text{des}}) \qquad (11)$$

where $v_{\text{vho}}^{\text{des}}$, v_{vho} are the desired and actual forward velocities at the VLO, and K_p is the proportional gain. This is possible since we constraint $\dot{L}_{\text{VLO}} = 0$.

Fig. 4 shows the comparison between our VLO controller (L controller) and the traditional controller with step length modulation (stepping). The stepping controller failed for this optimized gait: the velocity and system energy start to diverge after couple steps. Our L controller can still stabilize the gait based on the VLO velocity feedback. The converged trajectories are significantly close to the ones from the trajectory optimization. Based on our numerical exploration on different optimized walking gaits, the VLO controller (with $K_p = 10$) can stabilize all reasonable optimized trajectories with switching from SSP to DSP based on foot height.

It is important to note that this stabilization law is a feedback planning on the leg length trajectory. The importance comes from not sticking with following fixed desired trajectories. The feedback planning becomes necessary for shifting from the aSLIP to the full robot. On the walking of the full robot, there are foot impacts causing energy loss. There are also model differences between the aSLIP and the full robot. The CoM of the pelvis is not located at the hip pitch, for which can cause system energy to change according to [9], when controlled as a fixed orientation. In other words, the problem of the discrepancy between the models is solved by the feedback planning and control.

IV. LINEAR INVERTED PENDULUM MODEL FOR LATERAL BALANCING

Our aSLIP model provides a trajectory generation and feedback control method for the sagittal plane walking. Since the vertical mass oscillation is small (Fig. 3 (e)), we posit that the canonical Linear Inverted Pendulum (LIP) dynamics can
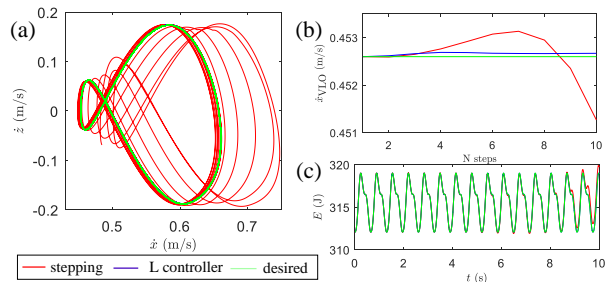

Fig. 4. Comparison between the stepping controller (changing step length) and our L controller (changing leg length) on the optimized aSLIP walking. (a) The phase portrait of the forward and vertical velocities of the mass. (b) The VLO velocities over 10 steps. (c) The system energy profiles over time.

serve as an approximation for the lateral rolling dynamics of the robot during 3D walking. Then a lateral stabilization method is designed to constantly plan lateral stepping during the Single Support Phase (SSP) to stabilize the system.

A. Linear Inverted Pendulum Dynamics

The Linear Inverted Pendulum (LIP) Model has been widely used for fully actuated humanoids in zero-moment-point (ZMP) walking [1]. Here, we only use the closed-form solution of the LIP to approximate the lateral rolling of the robot during walking. The LIP dynamics is purely passive,

$$\ddot{y}_c = \lambda^2 y_c \qquad (12)$$

where $\lambda = \sqrt{\frac{g}{z_0}}$, y_c is the lateral position and z_0 is the nominal height of the point mass. Fig. 5 (a) shows the diagram of the model. The closed form solution to this linear ODE is,

$$y_c = c_1 e^{\lambda t} + c_2 e^{-\lambda t}, \quad \dot{y}_c = \lambda(c_1 e^{\lambda t} - c_2 e^{-\lambda t}) \qquad (13)$$

where $c_1 = \frac{1}{2}(y_0 + \frac{1}{\lambda}\dot{y}_0)$ and $c_2 = \frac{1}{2}(y_0 - \frac{1}{\lambda}\dot{y}_0)$. y_0 and $\dot{y}_0$ is the initial condition of the LIP. Fig. 5 (b) shows the phase portrait of the system. The asymptotes, i.e. two straight lines (with slope λ) partition the state space into four domains. For the lateral balancing, it is desirable to keep the system inside the left (I) or right region (II) during the SSP. The DSP and the alternation of stance foot can switch the system states from one region to the other.

Following the principle of symmetry, one may want the LIP states to be symmetric at the boundary conditions of the SSP, i.e. $y_{\text{SSP}}^- = y_{\text{SSP}}^+, \dot{y}_{\text{SSP}}^- = -\dot{y}_{\text{SSP}}^+$, where the superscript $+$ and $-$ represent the beginning and the end of the SSP respectively. Given the duration of the SSP T_{SSP}, the boundary conditions satisfy,

$$\dot{y}_{\text{SSP}}^\pm = \pm \frac{\lambda \sinh(\frac{T_{\text{SSP}}}{2}\lambda)}{\cosh(\frac{T_{\text{SSP}}}{2}\lambda)} y_{\text{SSP}}^\pm := \pm \sigma y_{\text{SSP}}^\pm, \qquad (14)$$

which represent two straight lines in the phase diagram (see Fig. 5 (c)), and the slope σ of the straight lines increases with T_{SSP}. This indicates non-unique solutions for the lateral periodic motion for the LIP model. Given a desired

---

[2]The leg length dynamics is decoupled from the rest of the system. A linear controller is applied on $\ddot{L}$ to track the desired output trajectories $[L(t); \dot{L}(t)]$
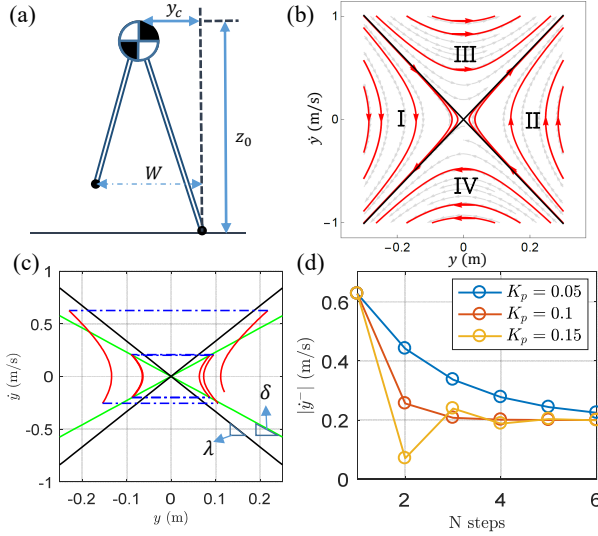
Fig. 5. (a) The Linear Inverted Pendulum (LIP) Model. (b) The phase portrait of the LIP dynamics. (c) Simulation of the feedback stepping on the ideal LIP stepping model from $y_0 = 0.12, \dot{y} = -0.15$. The desired boundary velocity is $\left|\dot{y}^-\right| = 0.2$. $T_{\text{DSP}} = 0.15s$, $T_{\text{SSP}} = 0.5s$. (d) The convergence of the stepping controller with different gains K_p.

step width W_s, the desired boundary condition of the SSP satisfies,

$$\left|\overline{\dot{y}_{\text{DSP}}}\right| T_{\text{DSP}} + 2\left|y_{\text{SSP}}^{\pm}\right| = W_s, \tag{15}$$

where $\overline{\dot{y}_{\text{DSP}}}$ is the averge velocity of $\dot{y}$ in DSP. We assume $\overline{\dot{y}_{\text{DSP}}} = \dot{y}_{\text{SSP}}^-$ since the DSP is short. Eq. (15) and (14) together provide a desired boundary condition on $\left|\dot{y}_{\text{SSP}}^{\pm}\right|$:

$$\left|\dot{y}_{\text{SSP}}^{\pm}\right| = \frac{\sigma W_s}{2 + \sigma T_{\text{DSP}}}. \tag{16}$$

Given the predefined step width and walking periods $T_{\text{DSP}}, T_{\text{SSP}}$ from the forward walking, the LIP dynamics suggests a desired boundary condition on the point mass state of the SSP. The desired boundary condition is used as a desired target reference for control. Stabilization to the target is described in the next part.

B. Lateral Balancing via Feedback Stepping

The LIP dynamics is passive, so is the lateral roll of the full robot. The only input to stabilize the lateral periodic motion is the step width. Changing the step width will change y_{SSP}^+. As a consequence, we provide the feedback stepping law as,

$$W = \hat{y}_{\text{SSP}}^- + \hat{\dot{y}}_{\text{SSP}}^- \hat{T}_{\text{DSP}} + \frac{\hat{\dot{y}}_{\text{SSP}}^-}{\hat{\sigma}} - K_p(\hat{\dot{y}}_{\text{SSP}}^- - \dot{y}_{\text{SSP}}^{\pm}), \tag{17}$$

where K_p is the proportional gain and $\hat{}$ represents the estimation of the quantity for the full robot. The estimation will be described later in the output construction for the full robot. The first three terms in (17) together place the mass state on the straight line with slope $\hat{\sigma}$. The last feedback term is based on the fact that a smaller $\left|y_{\text{SSP}}^+\right|$ leads to a smaller $\left|\dot{y}_{\text{SSP}}^-\right|$ for the following SSP, vice versa. The feedback term is the opposite of conventional stepping regulation for forward

walking [8], i.e. larger step length for larger velocity. The reason is that lateral motion in SSP is preferably staying in lateral stepping region (the region I and II (Fig. 5 (b)) for zero average velocity in the lateral direction; $y_c(t)$ does not cross 0 in SSP. This further suggests a lower bound on W to place the state $[y_{\text{SSP}}^+, \hat{\dot{y}}_{\text{SSP}}]$ in the stepping region. The lower bound is,

$$\underline{W} > \hat{y}_{\text{SSP}}^- + \hat{\dot{y}}_{\text{SSP}}^- \hat{T}_{\text{DSP}} + \frac{\hat{\dot{y}}_{\text{SSP}}^-}{\lambda}. \tag{18}$$

The lower bound means the minimum step width to prevent robot rolling over the next stance foot, i.e. getting into the region III and IV in Fig. 5 (b), which won't be catastrophic but requires additional care to prevent the robot crossing its legs during the next lateral step. Figure 5 (c) and (d) show the application of the feedback law on the ideal LIP stepping, for which no estimation is needed. Fast convergence to the desired boundary velocity can be achieved with appropriate gains.

V. CONTROLLER SYNTHESIS FOR WALKING

The previous two sections have described our trajectory generations and feedback controls on the reduced order models. In this section, we demonstrate that the trajectories and feedback controls can be implemented as desired output trajectories for controlling the 3D walking of the underactuated robot Cassie. The desired output trajectories are further stabilized via a rapidly exponentially stabilizing control Lyapunov functions based Quadratic program (RES-CLF-QP), with constraints on the torque limits and ground reaction forces. One can view the feedback controller synthesis from the reduced order models as a "high-level controller" for constructing and modulating the desired output trajectories, and the RES-CLF-QP as the "low-level controller" for tracking these trajectories.

A. The Two-domain Hybrid System of Walking

We first describe the hybrid model of the 3D walking [19], [20] of the full robot Cassie. The Single Support Phase (SSP) and Double Support Phase (DSP) compose the domains of the system, i.e. $\mathcal{D} = \{\mathcal{D}_{SSP}, \mathcal{D}_{DSP}\}$. In DSP, two feet are in contact with the ground. It transits to SSP when the rear stance foot is about to lift off the ground (ground reaction normal force becomes 0). Thus the domain and associated guard [20] can be defined as:

$$\mathcal{D}_{\text{DSP}} := \{(q, \dot{q}, u) : h_{\text{DSP}}(q) = 0, F_z^{\text{Feet}}(q, \dot{q}, u) > 0\},$$
$$\mathcal{S}_{\text{DSP}\to\text{SSP}} := \{(q, \dot{q}, u) : h_{\text{DSP}}(q) = 0, F_z^{\text{swing}}(q, \dot{q}, u) = 0\},$$

where $h_{\text{DSP}}(q)$ is the set of holonomic constraints in DSP. As there is no impact at the transition to SSP, the reset map is an identity map.

In SSP, one foot is in contact with the ground while the other foot is in swing. The transition to DSP happens when the swing foot strikes the ground. Therefore, we define the domain and corresponding guard as:

$$\mathcal{D}_{\text{SSP}} := \{(q, \dot{q}, u) : P_z^{\text{Foot}}(q) > 0, F^{\text{stance}}(q, \dot{q}, u) > 0\},$$
$$\mathcal{S}_{\text{SSP}\to\text{DSP}} := \{(q, \dot{q}, u) : P_z^{\text{swing}}(q) = 0, v_z^{\text{swing}}(q, \dot{q}) < 0\}.$$

We model the impact between the feet and the ground as plastic impact, the reset map of which can be found in [19].

The continuous dynamics of the system for each domain can be obtained from (1) and (2). Finally, the hybrid control system of walking be described by the tuple:

$$\mathscr{HC} = (\Gamma, \mathcal{D}, \mathcal{U}, \mathcal{S}, \Delta, FG), \tag{19}$$

where comprehensive definitions of each element can be found in [20], [19].

B. Output Definition

To enable the walking behavior on the 3D full order robot, we define the outputs with desired reference trajectories for each domain of the hybrid control system. It is important to emphasize the outputs from the reduced order models.

Leg Length. The actuation on the aSLIP model comes in the form of leg length trajectories $L(t)$. The trajectories are used as the desired leg length trajectory $L^{\text{des}}(t)$ on the full robot. The springs on the full robot are expected to behave similarly to that of the spring-mass model when leg length is actuated accordingly from the aSLIP model.

Leg Angle. The aSLIP optimization also provides the leg angles of both stance and swing leg during periodic walking. Since the robot has toe pitch actuation, it is necessary to include the leg angles as desired outputs. We define the leg angle β_{stance} as the pitch angle of the line between the hip roll joint and the toe pitch joint. We also define the virtual leg angle as the leg angle with zero spring deflections. The virtual leg angle is only used on the swing leg to get rid of the springs oscillation effect on the output. So it is termed as β_{swing}. Note that, since the robot has compliant rotational springs inside the leg and the toe is small, stringent stance angle trajectory tracking is problematic. A downscaling factor is applied on the stance angle output.

Recall that the aSLIP optimization has constructed continuous periodic leg length and leg angle trajectories. Additional constructions of $L^{\text{des}}(t)$, $\beta^{\text{des}}(t)$ are not necessary except for the use of the feedback control law (8) and (9).

1) Outputs for DSP: With two feet contacting the ground, the robot needs 6 outputs to fully define its motion. As noted above, the left and right leg length are used. It is also desirable to have zero roll, pitch, yaw angles of the pelvis. Lastly, we use one of the stance angles. As a result, we define the outputs for DSP as:

$$\mathcal{Y}_{\text{DSP}}(q,t) = \begin{bmatrix} L_{\text{L}}(q) \\ L_{\text{R}}(q) \\ \beta_{\text{stance}}(q) \\ \phi_{\text{roll}}(q) \\ \phi_{\text{pitch}}(q) \\ \phi_{\text{yaw}}(q) \end{bmatrix} - \begin{bmatrix} L_{\text{L}}^{\text{des}}(t) \\ L_{\text{R}}^{\text{des}}(t) \\ \beta_{\text{stance}}(t) \\ 0 \\ 0 \\ 0 \end{bmatrix}. \tag{20}$$

2) Outputs for SSP: In SSP, we define 10 outputs since the robot has 10 actuators. The 6 outputs defined in DSP are continually selected. Additional 4 outputs are on the swing leg, which are the virtual leg angle, swing foot pitch and

yaw angles and the lateral swing foot position. Therefore, the outputs for SSP are defined as:

$$\mathcal{Y}_{\text{SSP}}(q,t) = \begin{bmatrix} L_{\text{L}}(q) \\ L_{\text{R}}(q) \\ \beta_{\text{stance}}(q) \\ \beta_{\text{swing}}(q) \\ y_{\text{swing}}(q) \\ \phi_{\text{roll}}(q) \\ \phi_{\text{pitch}}(q) \\ \phi_{\text{yaw}}(q) \\ \phi_{\text{pitch}}^{\text{swing}}(q) \\ \phi_{\text{yaw}}^{\text{swing}}(q) \end{bmatrix} - \begin{bmatrix} L_{\text{L}}^{\text{des}}(t) \\ L_{\text{R}}^{\text{des}}(t) \\ \beta_{\text{stance}}(t) \\ \beta_{\text{swing}}(t) \\ y_{\text{swing}}^{\text{des}}(t) \\ 0 \\ 0 \\ 0 \\ 0 \\ 0 \end{bmatrix}, \tag{21}$$

where $y_{\text{swing}}(q)$ is the lateral position of the swing foot. The desired lateral swing foot position $y_{\text{swing}}^{\text{des}}(t)$ is constantly constructed from the lateral step width W in (17). We use the pelvis position as the mass position of the LIP. The estimation of the pre-impact states is based on (13). The current lateral pelvis state y and $\dot{y}$ can also used as the estimated pre-impact states; the desired swing width is then a stated based feedback construction. The estimation of walking period $\hat{T}_{\text{SSP}}$ is the average of previous T_{SSP}^i; $\hat{T}_{\text{DSP}} = T_{\text{SSP}} + T_{\text{DSP}} - \hat{T}_{\text{SSP}}$. Since the actual periods in each domain deviate slightly from the durations of the aSLIP walking, the simple estimations work well. The desired swing foot position is then continuously constructed by a spline-based curve.

C. RES-CLF-QP

To exponentially drive the outputs to zero, one can apply the traditional feedback linearization control [21] on the nonlinear system. However, the applied torque u from the feedback linearization control does not utilize the natural dynamics of the system and may violate the physical constraints of the walking. This motivated the work presented in [13] to construct rapidly exponentially stabilizing control Lyapunov functions (RES-CLF) to stabilize the output dynamics exponentially at a chosen rate ε. The end result is an inequality condition on the constructed Lyapunov function, which is,

$$\dot{V}_\varepsilon(u) \leq -\frac{\gamma}{\varepsilon}V_\varepsilon(\eta), \tag{22}$$

with some $\gamma > 0$, and $\eta = [\mathcal{Y}; \dot{\mathcal{Y}}]$. Eq. (22) can be explicitly written as an affine condition on u:

$$A^{\text{CLF}}(q,\dot{q})u \leq b^{\text{CLF}}(q,\dot{q}). \tag{23}$$

Detailed derivations can be found in [13]. The inequality on u naturally inspires a quadratic program (QP) formulation for solving u. The cost of the QP can be minimizing a linearly combination of $u^T u$ and $\mu^T \mu^3$. Therefore the RES-CLF-QP can be formulated as,

$$u^* = \underset{u \in \mathbb{R}^m}{\text{argmin}} \quad u^T H(q,\dot{q})u + 2F(q,\dot{q})u$$
$$\text{s.t.} \quad A^{\text{CLF}}(q,\dot{q})u \leq b^{\text{CLF}}(q,\dot{q}), \tag{CLF}$$

[3] $\mu = \mathcal{L}_{\mathbf{f}} + \mathcal{A}u$ [21] [13], which is the auxiliary input on the feedback linearized dynamics, where $\mathcal{A}$ is the decoupling matrix, and $\mathcal{L}_{\mathbf{f}}$ is the Lie derivative.

where $H(q,\dot{q}) = \alpha \mathcal{A}^T \mathcal{A} + (1-\alpha)I$, $F(q,\dot{q}) = \alpha \mathcal{L}_{\mathbf{f}}^T \mathcal{A}$, and $0 \le \alpha \le 1$ is to balance the convergence and smoothness of the QP [22] [23].

D. Main Control Law

Here we present our final feedback control algorithm for 3D underactuated walking via reduced order models.

The lower level controller is the RES-CLF-QP, which respects the torque bounds, ground reaction force (GRF) constraints and holonomic constraints for each domain. For the purpose of the optimization formulation, we include the holonomic constraint forces $F_{h,v}$ as the inputs to the system and as additional optimization variables in the QP. Then it is easy to encode the holonomic constraints as equality constraints and GRF as inequality constraints in the QP. The final QP-based controller for each domain $v \in V$ is:

$$\bar{u}_v^* = \underset{\bar{u}_v \in \mathbb{R}^{m+n_{h,v}}, \delta \in \mathbb{R}}{\operatorname{argmin}} \quad \bar{u}_v^T H_v \bar{u}_v + 2F_v \bar{u}_v + p\delta^2 \qquad (24)$$

$$\text{s.t.} \quad A_v^{\text{CLF}}(q,\dot{q})\bar{u}_v \le b_v^{\text{CLF}}(q,\dot{q}) + \delta, \quad \text{(CLF)}$$

$$A_v^{\text{GRF}}\bar{u}_v \le b_v^{\text{GRF}}, \qquad\qquad \text{(GRF)}$$

$$u_{lb} \le u \le u_{ub}, \qquad\qquad \text{(Torque)}$$

$$A_{h,v}(q,\dot{q})\bar{u}_v = b_{h,v}(q,\dot{q}). \text{(Holonomic)}$$

where $\bar{u}_v = [u; F_{h,v}]$. The formulation of each constraint can be found in [12]. A relaxation term δ is used on the CLF constraint to increase the feasibility of the QP. In implementation, we find that the relaxation term may temporarily compromise the convergence rate of the output tracking, but the overall convergence can still be achieved with a large positive penalty constant p.

The high level controller, which can also be viewed as a feedback planning method, includes the sagittal part for forward walking and the lateral part for balancing. The sagittal part is the modulation of the desired leg length trajectories by Eq. (8) and (9). The feedback is the forward velocity of the pelvis at the VLO. The lateral part is the continuous planning of the step width in SSP by Eq. (17). The feedback is the pelvis state $y_c, \dot{y}_c$ relative to its stance foot. Algorithm 1 shows the final feedback control law.

VI. Simulation Results

The proposed feedback control method is primarily implemented in simulation of the 3D underactuated bipedal robot Cassie shown in Fig. 1. The dynamics is numerically integrated using MATLAB's ode113 function with event functions. The QP is formulated and solved every at 0.5ms using qpOASES [24].

The simulation routine mainly follows that in Algorithm 1. Desired walking behavior is first described by step length, width and duration ranges of each domain. We use aSLIP trajectory optimization to find periodic solution of leg length and leg angle trajectories, along with the exact optimized durations of each domain. The desired boundary condition for the pelvis lateral states in SSP is then calculated from the LIP model. Then the simulation is started from an initial static standing configuration q_0 of the robot. In order to

---

Algorithm 1 The Feedback Control Law

Input: Desired behavior: step length and width, durations
1: $L(t), \beta(t), T_{\text{SSP}}, T_{\text{DSP}} \leftarrow$ aSLIP optimization
2: $\dot{y}_{\text{des}}$ from Eq. (16),
3: $\Gamma = 1$
4: **while** Simulation/Control loop **do**
5:    **if** SSP **then**
6:       $y_{\text{swing}}^{\text{des}}(t) \leftarrow$ Eq. (17)
7:       **if** VLO **then**
8:          $\Gamma \leftarrow$ Eq. (11)
9:       **end if**
10:   **end if**
11:   $L(t), \dot{L}(t) \leftarrow$ Eq. (8) (9)
12:   $\mathcal{Y}_{\text{SSP/DSP}}^{\text{des}}(t) \leftarrow t$,
13:   $u \leftarrow$ Eq. (24)
14: **end while**

---

initiate walking toward the desired behavior, we apply two SLIP models for the initial DSP and SSP before the periodic walking. The desired output trajectories are constructed similarly as the walking.

Fig. 6 shows the simulation results. The walking is not like conventional underactuated walking in that it does not converge to an orbit exactly; it converges to a stable region. The reason may come from the fact that the QP is solved discretely and the springs increase certain numerical errors in the process. Despite that, the spring forces resemble the ground reaction force well. The forward velocity is stabilized to the desired VLO velocity. Lateral boundary velocities converge to the desired value 0.2m/s. Overall, the walking behaves like that of the aSLIP and the lateral balancing converges like the LIP stepping.

VII. Conclusion and Future Work

In this paper, we present a feedback planning and control methodology for controlling walking on a 3D highly underactuated bipedal robot Cassie via reduced order models. The trajectory feedback planning consists a leg length feedback planning from our aSLIP model and a lateral stepping planning from the LIP model. The low level control for trajectory tracking is achieved using optimization-based control.

Future work will be devoted to the experiment implementation on the physical robot. The authors would also like to extend this feedback control method to general bipedal robots with or without compliance or foot actuation for generating various periodic locomotion behaviors. Theoretical guarantees will be to developed for understanding the stability of the walking achieved from coupled reduced order models.

References

[1] S. Kajita, F. Kanehiro, K. Kaneko, K. Fujiwara, K. Harada, K. Yokoi, and H. Hirukawa, "Biped walking pattern generation by using preview control of zero-moment point," in *Robotics and Automation, IEEE International Conference on*, vol. 2, 2003, pp. 1620–1626.

[2] J. Pratt, T. Koolen, T. De Boer, J. Rebula, S. Cotton, J. Carff, M. Johnson, and P. Neuhaus, "Capturability-based analysis and control of legged locomotion, part 2: Application to m2v2, a lower-body humanoid," *The International Journal of Robotics Research*, vol. 31, no. 10, pp. 1117–1133, 2012.
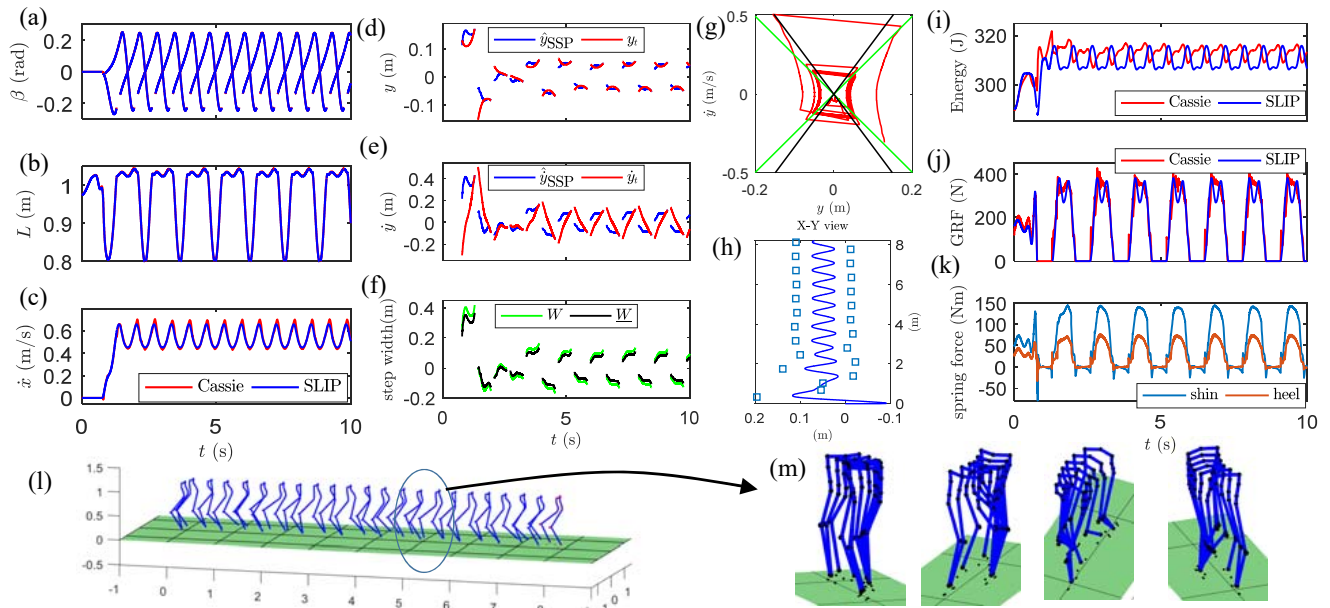
Fig. 6. Simulation results. (a, b, c) Leg angle, left leg length and forward velocity of the controlled walking of Cassie vs. these from the aSLIP walking. The discontinuity of the leg angle is due to that only one leg angle is used as the output in the DSP. (d, e, f) Lateral stepping results in terms of estimated preimpact states ($\hat{y}_{\text{SSP}}$, $\hat{\dot{y}}_{\text{SSP}}$) vs. current states ($y_t$, $\dot{y}_t$) and desired step width trajectory in SSP. (g) The phase plot of the pelvis position and velocity in the lateral direction. (h) The foot step location and the horizontal trajectory of the pelvis of Cassie. (i, j) Comparison of Cassie walking vs. aSLIP walking in terms of the total energies and vertical ground reaction forces on the left leg. (k) The spring joint torques on the left leg. (l, m) The snapshots of the walking.

[3] H. Geyer, A. Seyfarth, and R. Blickhan, "Compliant leg behaviour explains basic dynamics of walking and running," *Proceedings of the Royal Society of London B: Biological Sciences*, vol. 273, no. 1603, pp. 2861–2867, 2006.

[4] M. Ahmadi and M. Buehler, "Controlled passive dynamic running experiments with the arl-monopod ii," *IEEE Transactions on Robotics*, vol. 22, pp. 974–986, 2006.

[5] J. Rummel, Y. Blum, H. M. Maus, C. Rode, and A. Seyfarth, "Stable and robust walking with compliant legs," in *Robotics and automation (ICRA), 2010 IEEE international conference on*. IEEE, 2010, pp. 5250–5255.

[6] G. Garofalo, C. Ott, and A. Albu-Schäffer, "Walking control of fully actuated robots based on the bipedal slip model," *2012 IEEE International Conference on Robotics and Automation*, pp. 1456–1463, 2012.

[7] I. Poulakakis and J. Grizzle, "The spring loaded inverted pendulum as the hybrid zero dynamics of an asymmetric hopper," *IEEE Transactions on Automatic Control*, vol. 54, no. 8, pp. 1779–1793, 2009.

[8] M. H. Raibert, *Legged robots that balance*. MIT press, 1986.

[9] S. Rezazadeh and et al., "Spring-mass walking with atrias in 3d: Robust gait control spanning zero to 4.3 kph on a heavily underactuated bipedal robot," in *ASME 2015 dynamic systems and control conference*. American Society of Mechanical Engineers, 2015.

[10] A. Hereid, M. J. Powell, and A. D. Ames, "Embedding of slip dynamics on underactuated bipedal robots through multi-objective quadratic program based control," in *Decision and Control (CDC), 2014 IEEE 53rd Annual Conference on*. IEEE, pp. 2950–2957.

[11] M. J. Powell and A. D. Ames, "Mechanics-based control of underactuated 3d robotic walking: Dynamic gait generation under torque constraints," in *Intelligent Robots and Systems (IROS), 2016 IEEE/RSJ International Conference on*. IEEE, 2016, pp. 555–560.

[12] X. Xiong and A. D. Ames, "Bipedal hopping: Reduced-order model embedding via optimization-based control," in *IEEE/RSJ International Conference on Intelligent Robots and Systems, IROS 2018, Spain, https://arxiv.org/pdf/1807.08037.pdf*.

[13] A. D. Ames, K. Galloway, K. Sreenath, and J. Grizzle, "Rapidly exponentially stabilizing control lyapunov functions and hybrid zero dynamics," *IEEE Transactions on Automatic Control*, vol. 59, no. 4, pp. 876–891, 2014.

[14] Agility Robotics http://www.agilityrobotics.com.

[15] C. Hubicki, J. Grimes, M. Jones, D. Renjewski, A. Spröwitz, A. Abate, and J. Hurst, "Atrias: Design and validation of a tether-free 3d-capable spring-mass bipedal robot," *The International Journal of Robotics Research*, vol. 35, no. 12, pp. 1497–1521, 2016.

[16] A. Hereid, E. A. Cousineau, C. M. Hubicki, and A. D. Ames, "3d dynamic walking with underactuated humanoid robots: A direct collocation framework for optimizing hybrid zero dynamics," in *Robotics and Automation (ICRA), 2016 IEEE International Conference on*. IEEE, 2016, pp. 1447–1454.

[17] C. M. Hubicki, J. J. Aguilar, D. I. Goldman, and A. D. Ames, "Tractable terrain-aware motion planning on granular media: an impulsive jumping study," in *Intelligent Robots and Systems (IROS), 2016 IEEE/RSJ International Conference on*. IEEE, 2016, pp. 3887–3892.

[18] X. Da, O. Harib, R. Hartley, B. Griffin, and J. Grizzle, "From 2d design of underactuated bipedal gaits to 3d implementation: Walking with speed tracking," *IEEE Access*, vol. 4, pp. 3469–3478, 2016.

[19] J. Grizzle, C. Chevallereau, R. W. Sinnet, and A. D. Ames, "Models, feedback control, and open problems of 3d bipedal robotic walking," *Automatica*, vol. 50, no. 8, pp. 1955–1988, 2014.

[20] A. D. Ames, "Human-inspired control of bipedal walking robots," *IEEE Transactions on Automatic Control*, vol. 59, no. 5, pp. 1115–1130, 2014.

[21] H. K. Khalil, "Noninear systems," *Prentice-Hall, New Jersey*, vol. 2, no. 5, pp. 5–1, 1996.

[22] B. Morris, M. J. Powell, and A. D. Ames, "Sufficient conditions for the lipschitz continuity of qp-based multi-objective control of humanoid robots," in *Decision and Control (CDC), 2013 IEEE 52nd Annual Conference on*. IEEE, 2013, pp. 2920–2926.

[23] B. J. Morris, M. J. Powell, and A. D. Ames, "Continuity and smoothness properties of nonlinear optimization-based feedback controllers," in *Decision and Control (CDC), 2015 IEEE 54th Annual Conference on*. IEEE, 2015, pp. 151–158.

[24] H. Ferreau, C. Kirches, A. Potschka, H. Bock, and M. Diehl, "qpOASES: A parametric active-set algorithm for quadratic programming," *Mathematical Programming Computation*, vol. 6, no. 4, pp. 327–363, 2014.